Sintering and characterisation of $Gd_3Al_3Ga_2O_{12}/Y_3Al_5O_{12}$ layered composite scintillation ceramic

Xianqiang Chen[a,b], Haiming Qin[a,*], Xinjia Wang[a], Chengrui Yang[a], Jun Jiang[a,*], Haochuan Jiang[a,*]

[a] *Ningbo Institute of Materials Technology and Engineering, Chinese Academy of Sciences, Ningbo 315201, China*
[b] *University of Chinese Academy of Science, Beijing 100039, China*

ARTICLE INFO

Keywords:
Scintillation ceramic
Layered GGAG/YAG
Low temperature sintering
Spectra designation

ABSTRACT

A novel layered GGAG/YAG composite scintillation ceramic can be prepared at 1650 °C using an easily accessible preparation procedure. The oxygen sintering-hot isostatic pressing method implemented in this work can significantly shorten the preparation period of scintillation ceramics. The ceramic exhibits regular grain microstructure. Interface of the composite ceramic is clean and straight. As prepared, the layered Ce:GGAG/Cr:YAG composite ceramic can emit a broad range of photons with wavelength from 500 to 750 nm under excitation. The integral spectra is composed of three parts: emitted photons of Cr:YAG and Ce:GGAG and emitted light of Cr:YAG excitated by the photons emitted by the Ce:GGAG ceramic layerprepared by the proposed method. The method accomplished in this work can significantly improve the exploration of full spectrum scintillation/luminescence ceramics preparation and spectra designation.

1. Introduction

Ceramic scintillators have many advantages compared with single crystal scintillators such as more uniform doping, easier preparation procedure and lower cost for batch production [1,2]. With the development of ceramic preparation techniques, ceramic scintillators have been well utilized for ionizing radiation detection, especially in the X-ray detection and nuclear medical diagnostics in the past two decades [3]. Using scintillators for commercial medical computed tomography (CT) systems for example, three ceramic scintillators: Eu:$(Y,Gd)_2O_3$ (usually known as HiLight) [4] and Ce:$(Lu,Tb)_3Al_5O_{12}$ (usually known as Gemstone) [5–7] were developed by GE Healthcare; Pr:Gd_2O_2S-based ceramic (GOS), first developed by researchers of Hitachi Company [8–10] were successfully applied as the detection unit for CT systems.

Aside from those traditional ceramic systems, researchers have attempted to explore new scintillators with high scintillation performance [11]. Among which, attempts accomplished by Cherepy and Kamada in $Re_3(Al,Ga)_5O_{12}$ garnet scintillators need to be emphasized [12–14]. Their work established and consolidated this material as new scintillators with extraordinary performance. Ce-doped $Gd_3(Al,Ga)_5O_{12}$ (Ce:GGAG) single crystal scintillator exhibited light yield as high as 55,000 photons/MeV coupled with an energy resolution of about 3.7% at 662 keV [15]. Outstanding chemical and physical properties such as refractory nature, high density (>6 g/m^3) and good scintillation properties of Ce:GGAG-based materials make these materials particularly attractive for Positron Emission Tomography (PET) and other γ-ray detection applications [14–17].

Yttrium aluminum garnet (YAG) material is also attractive as matrix of laser medium and luminescent material due to its excellent chemical and physical properties [18–20]. YAG-based luminescent materials are of the most widely investigated luminescent materials. YAG matrix has several favorable properties such as the physical, chemical stability, and transparency over a broad spectral range.

In view of their cubic crystalline structure, GGAG and YAG are feasible for the preparation of transparent ceramics. Homogeneous doping of active ions over a single crystal is difficult because of the segregation coefficient of active ion element in a single crystal matrix [21]. Besides, the growth of single crystal with the Czochralski method, taking YAG for example, has many drawbacks, such as its low growth rate and expensive equipment is required. Commercial Nd:YAG single crystals are grown at approximately 2000 °C for a growth period about 1000–2000 h [18]. At the same time, the

* Corresponding authors.
E-mail addresses: qinhaiming@nimte.ac.cn (H. Qin), jjun@nimte.ac.cn (J. Jiang), jianghaochuan@nimte.ac.cn (H. Jiang).

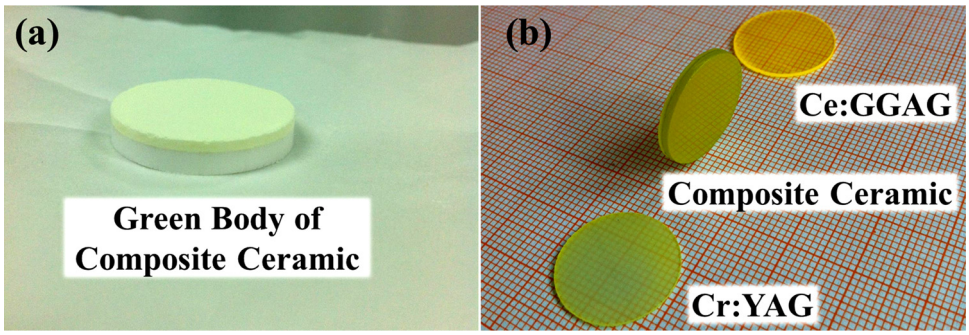

Fig. 1. Picture for (a) green body of Ce:GGAG/Cr:YAG composite ceramic (b) sintered sample of Cr:YAG, layered Ce:GGAG/Cr:YAG composite ceramic and Ce:GGAG. (For interpretation of the references to colour in this figure legend, the reader is referred to the web version of this article.)

core which locates in the central region of the single crystal ingot and facets arised from the central region to the outer region limit the utilization efficiency of single crystals. Fortunately, with the technique developed utilizing transparent ceramics, transparent ceramic have become a promising substitution for the single crystal technique.

Our group also tried the preparation of a garnet ceramic system and successfully obtained ceramics with high transparency and outstanding scintillation performance [22–25]. In present work, we proposed a novel layered GGAG/YAG composite scintillation ceramics prepared at the temperature of 1650 °C, which is a relatively low temperature compared with traditional preparation temperature of garnet ceramics such as $Y_3Al_5O_{12}$ and $Lu_3Al_5O_{12}$ etc (about 1750 °C or even higher) [18,28–30]. The ceramic is designed with layered structure where different luminescence center were accommodated individually. Ce and Cr ions were accommodated in different layers to form complementary spectra component. They can emit photons with different energies under high energy excitation. The method accomplished in this work can significantly improve the exploration of full spectrum scintillation/luminescence ceramic preparation and spectra designations. That will make the detection of scintillation photons easier since expansion of scintillation spectra can better agree with the optimal response interval of detectors such as silicon diodes. Besides, spacial separated luminescent centers in individual matrix avoid the mutual interaction of co-doped luminescent centers in same confined crystalline structure. Individual mediation on each component of the layered structure can be easily accomplished by varying its layered structure dimension scale and luminescent centers' concentration. Density difference of each layer (ρ_{GGAG} = 6.5 g/cm^3 ρ_{YAG} = 4.5 g/cm^3) can also offer possibility of adjustment of overall density of the composite ceramic from 4.5–6.5 g/cm^3 [18,24]. That means the composite ceramic can meet the requirement for the application in a wide X-ray energy range.

2. Experiment

Commercial Gd_2O_3, Ga_2O_3 (99.99%, GanZhou QianDong Rare Earths Group Co., Ltd., China), Y_2O_3 (99.9%, Rare-chem Hi-tech Co., Ltd., China), Al_2O_3 (99.99%, Taimei Chemicals Co., Ltd., Japan) Cr_2O_3 and CeO_2 (99.9%, Beijing Dk Nano technology Co., LTD., China) powders were used as the starting materials. Gd_2O_3, Ga_2O_3, Al_2O_3 and Y_2O_3 powders were calcined at 600 °C and 1000 °C, respectively, for 2 h to remove moisture. The powders were weighed according to the composition of $Ce_{0.015}Gd_{2.985}Al_3Ga_2O_{12}$ (Ce:GGAG) and $Cr_{0.025}Y_3Al_{4.975}O_{12}$ (Cr:YAG). No sintering aid was added. After a mixture process by ball milling (corundum ball mill with W_{ball}/W_{powder} = 10:1) for 12 h in alcohol at the rotation speed of 300 rpm, mixed powders were dried, calcined, then dry-pressed into 25 mm diameter pellets and cold isostatically pressed under a pressure of 250 MPa. Green body of GGAG/YAG composite ceramics were prepared by sequential bedding of each powders. No binder was used for the forming process. The compacted powder was sintered at 1650 °C for 2 h in flowing dry oxygen gas at 0.6 L/min. A hot isostatic pressing process was performed to further consolidate the sample (200 Mpa in Ar atmosphere, 1650 °C/2 h). Finally the disk specimens of ~20 mm in diameter were mirror-polished on both surfaces thermally etched at 1300 °C for 30 min for grain size measurement and other characterisations.

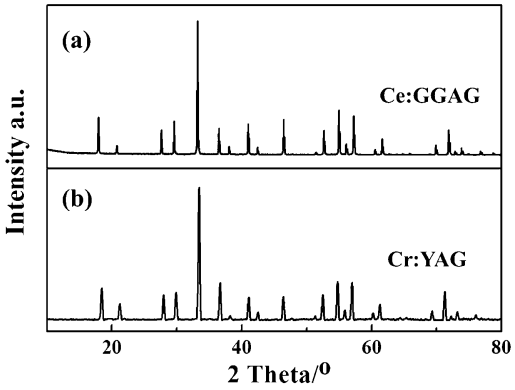

Fig. 2. X-ray diffraction pattern of Ce:GGAG and Cr:YAG sintered at 1650 °C.

Phase information of the samples was identified by X-ray diffraction (XRD, Model D8 Advance, Bruker AXS Co., Germany) using CuKα radiation in the range of 2θ = 10°–80°. Morphologies of the ceramics were examined by scanning electron microscopy (SEM, Quanta FEG 250, FEI Co., USA). Grain size of the sintered samples was obtained by the linear intercept method (200 grains included). The average grain size was calculated by multiplying the average linear intercept distance by 1.56. The optical transmittance was measured with a spectrometer (Lambda 950, Perkin Elmer Co., USA) in 200–800 nm range. Excitation and emission spectra were measured at room temperature with a fluorescence spectrometer (F-4600, Hitachi, Tokyo, Japan).

3. Results and discussion

Fig. 1a presents the picture for the green body of Ce:GGAG/Cr:YAG composite ceramic. It can be seen from the figure that the layered structure can be obtained via a cold isostatic press process after mold moulding. Fig. 1b shows the image for sintered sample of Cr:YAG, layered Ce:GGAG/Cr:YAG composite ceramic and Ce:GGAG from bottom to top. All samples show good transparency.

Fig. 2 shows the X-ray diffraction pattern of Ce:GGAG and Cr:YAG sample sintered at 1650 °C. All observed peaks of Ce:GGAG

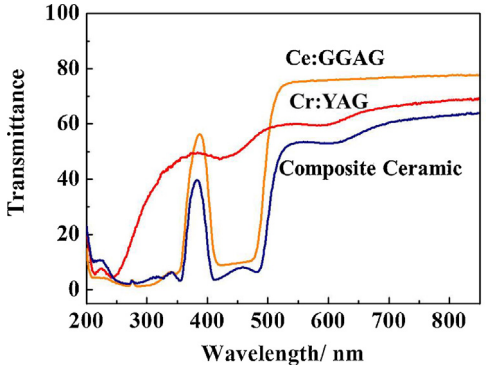

Fig. 3. Optical transmittance of polished sample of Cr:YAG, layered Ce:GGAG/Cr:YAG composite and Ce:GGAG ceramics.

and Cr:YAG from 10° to 80° can be indexed to the standard diffractions pattern of pure $Gd_3Ga_2Al_3O_{12}$ (JCPDS no. 46–0448) and $Y_3Al_5O_{12}$ (JCPDS no. 33–40), respectively. No other phases were detected according to the XRD patterns. That indicates the accomplishment of GGAG and YAG crystalline structure during the preparation procedure.

Fig. 3 presents the transmittance of Cr:YAG, Ce:GGAG/Cr:YAG composite and Ce:GGAG ceramics. Among which, Ce:GGAG sample exhibits the highest transmittance. At the wavelength of above 550 nm, which is the main emission range of Ce:GGAG, the transmittance is up to 77%. While Cr:YAG and layered Ce:GGAG/Cr:YAG composite ceramic can reach transmittance over 60% and 50%, respectively, at the wavelength around 550 nm. Their transmittance can be even higher in the long band region. The inferior transmittance of Ce:GGAG/Cr:YAG composite ceramic is mainly ascribed to the difference between the refractive indices of YAG and GGAG phase, which will cause light scattering and decrease of the transmittance. The absorption bands of Ce:GGAG ceramic around 350 nm and 450 nm can be attributed to $4f \rightarrow 5d_2$ and $4f \rightarrow 5d_1$ transition of Ce^{3+}, respectively [23]. While the absorption bands of Cr:YAG ceramic around 250 nm, 450 nm and 610 nm can be attributed to $^4A_2(^4F) \rightarrow {}^4T_1\,(^4P)$, $^4A_2\,(^4F) \rightarrow {}^4T_1\,(^4F)$, and $^4A_2\,(^4F) \rightarrow {}^4T_2\,(^4F)$ transition of Cr^{3+} [26]. Transmittance spectrum of Ce:GGAG/Cr:YAG composite ceramic exhibits the absorption bands of Cr:YAG and Ce:GGAG ceramics, those bands can be attributed to electronic transition of Ce^{3+} and Cr^{3+} as described before.

Fig. 4 shows the microstructures of the thermal etched samples. It can be seen from Fig. 4a and b that both Ce:GGAG and Cr:YAG show regular grain structure and grain boundaries. However, the grain sizes of these two samples differ greatly. Average grain size D can be determined by linear intercept method (200 grains counted). The average grain size of Ce:GGAG is about 5 μm while that of Cr:YAG ceramic is about 2–3 μm. Fig. 4c and d show the interface

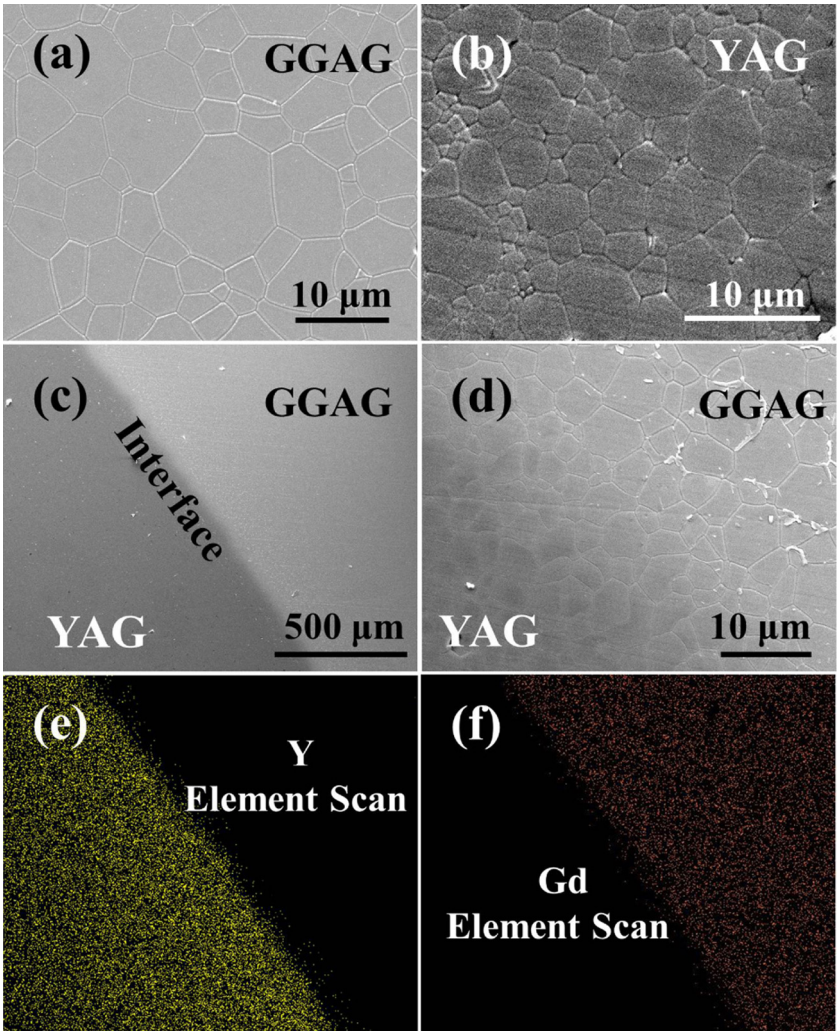

Fig. 4. Microstructures of the thermal etched samples: (a) Ce:GGAG ceramic, (b) Cr:YAG ceramic, (c) and (d) layered Ce:GGAG/Cr:YAG composite ceramic, (e) and(f) EDS mapping analysis of Ce:GGAG/Cr:YAG composite ceramic.

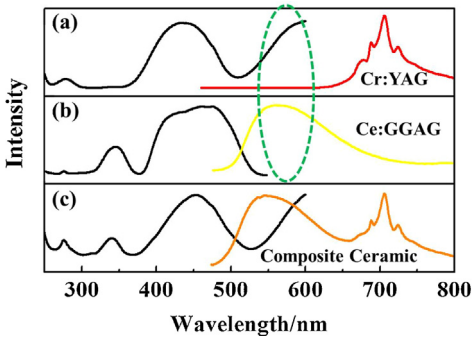

Fig. 5. Room temperature excitation-emission spectra of (a) Cr:YAG, (b) Ce:GGAG (c) layered Ce:GGAG/Cr:YAG composite ceramic.

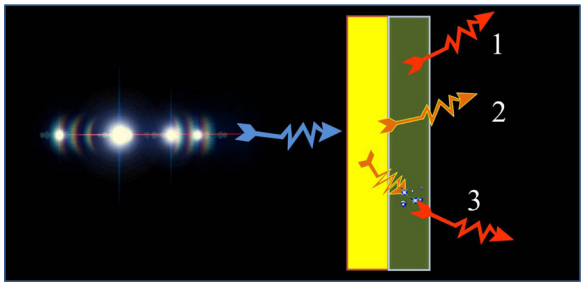

Fig. 6. Schematic illustration of the emission process of the as prepared Ce:GGAG/Cr:YAG composite ceramic.

microstructure of Ce:GGAG/Cr:YAG composite ceramic. The interface is clean and straight. The contrast of different ceramics can be attributed to the atomic weight difference of Ce:GGAG and Cr:YAG elements. Thickness of the interface is only about 10–20 μm. Precise control of the interface can help with the reduction of photon loss during its transmission procedure. Fig. 4e and f present the EDS mapping analysis of Ce:GGAG/Cr:YAG composite ceramic. It can be seen from the figure that Y element and Gd elements distribute separately along the interface. The result indicates that the absolutely separated ceramic matrix was accomplished by controlling its element diffusion.

Fig. 5 shows the room temperature excitation-emission spectra of (a) Cr:YAG, (b) Ce:GGAG (c) layered Ce:GGAG/Cr:YAG composite ceramic. For the Ce:GGAG sample the excitation spectrum was monitored at the emission maxima of the Ce^{3+} emission at about 558 nm (5d-4f transition), the emission spectrum was measured for excitation at 469 nm [23,24]. The excitation spectra are consistent with the optical transmittance curves presented in Fig. 3. Cr:YAG phosphor can be sufficiently excited at the excitation wavelength of around 438 nm. Its main emission peaks around 700 nm, which is consistent with the typical emission spectra of Cr ion (^4T-^2A transition) in YAG matrix [27].

Fig. 5c shows the excitation-emission spectra of Ce:GGAG/Cr:YAG composite ceramic. It can be seen from the spectra that the composite ceramic exhibits the excitation-emission behaviors of Cr:YAG and Ce:GGAG ceramics. A broad range of emission spectra can be obtained from 500 to 750 nm in the composite ceramic. We can see from Fig. 5 that the excitation spectra of Cr:YAG overlaps with emission spectra of Ce:GGAG. It indicates that the Cr:YAG layer can be excited by both the excitation source and the emission photons of Ce:GGAG. Similar phenomenon was also proved by Wang, etc in Cr and Ce co-doped YAG phosphor in 2008 [27].

Schematic illustration of the emission process of the as prepared Ce:GGAG/Cr:YAG composite ceramic is shown in Fig. 6. After the formation of the layered composite ceramic, under the excitation of photon with wavelength of 460 nm, the layered composite ceramic can emit photons with wavelength ranges from 500 to 750 nm. Based on the experiment and explanation above, we can conclude that the emitted photons include three parts: clearly, the first two portions of the integral spectra are from the emission photons of Ce:GGAG and Cr:YAG respectively, and a third portion of the integral spectra are of the emission photons of Cr:YAG excited by the emission photons of Ce:GGAG layer. Expansion of scintillation spectra will make the detection of scintillation photons easier since it can better agree with the optimal response interval of detectors.

4. Conclusion

Novel layered GGAG/YAG bilayer composite scintillation ceramic can be prepared at 1650 °C in oxygen and followed by hot isostatic pressing at 1650 °C and 200 Mpa in Ar atmosphere for 2 h. The ceramic exhibits regular and uniform grains. The average grain size of Ce:GGAG is about 5 μm while that of Cr:YAG ceramic is about 2–3 μm. Interface of the composite ceramic is clean and straight. As prepared, layered Ce:GGAG/Cr:YAG composite ceramic can emit a broad range of photons with wavelengths from 500 to 750 nm. Individual mediation on each component of the layered structure can be easily accomplished by varying its layered structure dimension scale and luminescent centers' concentration. Density difference of each layer (ρ_{GGAG} = 6.5 g/cm^3 ρ_{YAG} = 4.5 g/cm^3) can also offer the possibility of adjustment of overall density of the composite ceramics.

Acknowledgements

This research was supported by NSFC (51502308, 51402317), Project of Technology Application for Public Welfare of Zhejiang Province (2016C31028), and Ningbo Science and Technology Innovation Team (Grant No. 2014B82004). The authors are grateful to Mr. Ron George and Mrs. George for language revision of the manuscript.

References

[1] C. Greskovich, S. Duclos, Ceramic scintillators, Annu. Rev. Mater. Sci. 27 (1) (1997) 69–88.
[2] D.J. Wisniewski, L.A. Boatner, J.S. Neal, G. Jelison, Development of novel polycrystalline ceramic scintillators, IEEE Nucl. Sci. 55 (3) (2008) 1501–1508.
[3] M. Nikl, Scintillation detectors for X-rays, Meas. Sci. Technol. 17 (4) (2006) R37.
[4] C.D. Greskovich, D. Cusano, D. Hoffman, R.J. Riedner, Ceramic scintillators for advanced, medical X-ray detectors, Am. Ceram. Soc. Bull. 71 (7) (1992) 1120–1130.
[5] G.E. Novel, Scintillator delivers CT imaging revolution, Am. Ceram. Soc. Bull. 89 (8) (2010) 43–44.
[6] J. Vartuli, R. Lyons, C. Vess, K. Mecvoy, R. Hagerdon, S. Duclos, GE Healthcare's New Computed Tomography Scintillator-Gemstone, Presentation at SORMA, San Diago, 2008.
[7] H. Jiang, J. Vartuli, C. Vess, Gemstone—The Ultimate Scintillator for Computed Tomography, GE White Paper, CT-0376-1108-EN-US, (2008).
[8] Y. Ito, H. Yamada, M. Yoshida, H. Fujii, G. Toda, H. Takeuchi, Y. Tsukuda, Hot isostatic pressed Gd_2O_2S: Pr, Ce, F translucent scintillator ceramics for X-ray computed tomography detectors, Jpn. J. Appl. Phys. 27 (8A) (1988) L1371.
[9] H. Yamada, A. Suzuki, Y. Uchida, M. Yoshida, H. Yamamoto, Y. Tsukuda, A scintillator Gd_2O_2S: Pr, Ce, F for X-ray computed tomography, J. Electrochem. Soc. 136 (9) (1989) 2713–2716.
[10] M. Yoshida, M. Nakagawa, H. Fujii, F. Kawaguchi, H. Yamada, Y. Ito, Application of Gd_2O_2S ceramic scintillator for X-ray solid state detector in X-ray CT, Jpn. J. Appl. Phys. 27 (8A) (1988) L1572.
[11] M. Nikl, A. Yoshikawa, K. Kamada, K. Nejezchleb, C.R. Stanek, J.A. Mares, K. Blazek, Development of LuAG-based scintillator crystals—a review, Prog. Cryst. Growth Charact. 59 (2) (2013) 47–72.
[12] N.J. Cherepy, S.A. Payne, B.W. Sturm, J.D. Kuntz, Z.M. Seeley, B.L. Rupert, R.D. Sanner, O.B. Drury, T.A. Hurst, S.E. Fisher, M. Groza, L. Matei, A. Burger, R. Hawrami, K.S. Shah, L.A. Boatner, Comparative gamma spectroscopy with SrI_2(Eu), GYGAG(Ce) and Bi-loaded plastic scintillators, IEEE Nuc. Sci. Symp. Conf. Record (2010) 1288–1291.
[13] N.J. Cherepy, J.D. Kuntz, Z.M. Seeley, S.E. Fisher, O.B. Drury, B.W. Sturm, T.A. Hurst, R.D. Scanner, J.J. Roberts, S.A. Payne, Transparent ceramic scintillators

for gamma spectroscopy and radiography, Proc. SPIE (2010), 78050I-1–78050I-5.
[14] K. Kamada, T. Endo, K. Tsutumi, T. Yanagida, Y. Fujimoto, A. Fukabori, A. Yoshikawa, J. Pejchal, M. Nikl, Composition engineering in cerium-doped (Lu,Gd)$_3$ (Ga,Al) 5O12 single-crystal scintillators, Cryst. Growth Des. 11 (10) (2011) 4484–4490.
[15] P. Sibczynski, J. Iwanowska-Hanke, M. Moszyński, L. Swiderski, M. Szawłowski, M. Grodzicka, T. Szczęśniak, K. Kamada, A. Yoshikawa, Characterization of GAGG:Ce scintillators with various Al-to-Ga ratio, Nucl. Instrum. Methods Phys. Res. Sect. A 772 (2015) 112–117.
[16] K. Kamada, T. Yanagida, T. Endo, K. Tsutumi, Y. Usuki, M. Nikl, Y. Fujimoto, A. Fukabori, A. Yoshikawa, 2inch diameter single crystal growth and scintillation properties of Ce:$Gd_3Al_2Ga_3O_{12}$, J. Cryst. Growth 352 (1) (2012) 88–90.
[17] Y. Wang, G. Baldoni, W.H. Rhodes, C. Brecher, A. Shah, U. Shirvadkar, Transparent garnet ceramic scintillators for gamma-ray detection, Proc. SPIE 8507 (2) (2012) 504–507.
[18] A. Ikesue, Y.L. Aung, Ceramic laser materials, Nat. Photonics 2 (12) (2008) 721–727.
[19] S. Chen, H. Wei, C.L. Melcher, Y. Wu, Spectroscopic properties of transparent $Y_3Al_5O_{12}$:Eu ceramics, Opt. Mater. Express 3 (12) (2013) 2022–2027.
[20] W. Chewpraditkul, L. Swiderski, M. Moszynski, T. Szczesniak, A. Syntfeld-Kazuch, C. Wanarak, P. Limsuwan, Comparative studies of $Lu_3Al_5O_{12}$:Ce and $Y_3Al_5O_{12}$:Ce scintillators for gamma-ray detection, Phys. Status Solidi A 206 (11) (2009) 2599–2605.
[21] B. Cockayne, M. Chesswas, D.B. Gasson, Facetting and optical perfection in Czochralski grown garnets and ruby, J. Mater. Sci. 4 (5) (1969) 450–456.
[22] H. Chen, Y. Qin, Z. Zhang, Y. Luo, J. Liu, H. Jiang, Fabrication of cerium-doped nonstoichiometric $(Ce,Lu,Gd)_{3+\delta}(Ga,Al)_{5-\delta}O_{12}$ transparent ceramics, J. Rare Earth 33 (8) (2015) 863–866.
[23] H. Chen, Y. Qin, Z. Zhang, J. Luo, H. Jiang, Preparation and optical properties of transparent $(Ce,Gd)Al_3Ga_2O_{12}$ ceramics, J. Am. Ceram. Soc. 98 (8) (2015) 2352–2356.
[24] X. Chen, H. Qin, Y. Zhang, J. Jiang, H. Jiang, Highly transparent ZrO_2-doped $(Ce,Gd)_3Al_3Ga_2O_{12}$ ceramics prepared via oxygen sintering, J. Eur. Ceram. Soc. 35 (14) (2015) 3879–3883.
[25] Z. Luo, H. Jiang, J. Jiang, R. Mao, Microstructure and optical characteristics of Ce:$Gd_3(Ga,Al)_5O_{12}$ ceramic for scintillator application, Ceram. Int. 41 (1) (2015) 873–876.
[26] J. Xu, J. Ueda, Y. Zhuang, B. Viana, S. Tanabe, $Y_3Al_{5-x}Ga_xO_{12}:Cr^{3+}$: a novel red persistent phosphor with high brightness, Appl. Phys. Express 8 (4) (2015) 042602.
[27] W.D. Wang, J.K. Tang, S.T. Hus, J. Wang, B.P. Sullivan, Energy transfer and enriched emission spectrum in Cr and Ce co-doped $Y_3Al_5O_{12}$ yellow phosphors, Chen. Phys. Lett. 457 (1) (2008) 103–105.
[28] H. Qin, J. Jiang, H. Jiang, Y. Sang, D. Sun, X. Zhang, J. Wang, H. Liu, Effect of composition deviation on the microstructure and luminescence properties of Nd:YAG ceramics, CrystEngComm 16 (2014) 10856–10862.
[29] J. Liu, X. Cheng, J. Li, T. Xie, M. Ivanov, X. Ba, H. Chen, Q. Liu, Y. Pan, J. Guo, Influence of non-stoichiometry on solid-state reactive sintering of YAG transparent ceramics, J. Eur. Ceram. Soc. 35 (2015) 3127–3136.
[30] N. Wagner, B. Herden, T. Dierkes, J. Plewa, T. Jüstel, Towards the preparation of transparent LuAG:Nd^{3+} ceramics, J. Eur. Ceram. Soc. 32 (2012) 3085–3089.